Iso-Risk Air No Decompression Limits after Scoring Marginal Decompression Sickness Cases as Non-Events

F. Gregory Murphy[1,2], Ashleigh J. Swingler[1], Wayne A. Gerth[2], Laurens E. Howle[1,3,4,†]

[1]Mechanical Engineering and Materials Science Department, Duke University, Durham, NC

[2]Navy Experimental Diving Unit, Panama City, FL

[3]Radiology Department, Duke University Medical Center, Durham, NC

[4]BelleQuant Engineering, PLLC, Mebane, NC

†Corresponding author: laurens.howle@duke.edu, 919.660.5336

Abstract

Decompression sickness (DCS) in humans is associated with reductions in ambient pressure that occur during diving, aviation, or certain manned spaceflight operations. Its signs and symptoms can include, but are not limited to, joint pain, radiating abdominal pain, paresthesia, dyspnea, general malaise, cognitive dysfunction, cardiopulmonary dysfunction, and death. Probabilistic models of DCS allow the probability of DCS incidence and time of occurrence during or after a given hyperbaric or hypobaric exposure to be predicted based on how the gas contents or gas bubble volumes vary in hypothetical tissue compartments during the exposure. These models are calibrated using data containing the pressure and respired gas histories of actual exposures, some of which resulted in DCS, some of which did not, and others in which the diagnosis of DCS was not clear. The latter are referred to as marginal DCS cases. In earlier works, a marginal DCS event was typically weighted as 0.1, with a full DCS event being weighted as 1.0, and a non-event being weighted as 0.0. Recent work has shown that marginal DCS events should be

weighted as 0.0 when calibrating gas content models. We confirm this indication in the present work by showing that such models have improved performance when calibrated to data with marginal DCS events coded as non-events. Further, we investigate the ramifications of derating marginal events on model-prescribed air diving no-stop limits.

Keywords

Hyperbaric, Deep Sea Diving, Marginal, Decompression Sickness, DCS, Gas Content, Inert Gas

Introduction

The signs and symptoms of decompression sickness (DCS) in humans, which is associated with reductions in ambient pressure during diving, aviation, or certain manned spaceflight operations, can include, but are not limited to joint pain, radiating abdominal pain, paresthesia, dyspnea, general malaise, cognitive dysfunction, cardiopulmonary dysfunction, and death [1, 2]. DCS is typically categorized as either type 1 pain only, or type 2 neurological [3, 4]. Our focus here is on the problem of DCS caused by decompressions from hyperbaric exposures, not decompressions to hypobaric pressures, such as those experienced by pilots on ascent to high altitudes and astronauts during extravehicular activities. Haldane *et al.* [5] are commonly credited with developing the first effective strategy for preventing DCS in man. The latter entailed tracking gas content in a series of independent compartments. Within each compartment, the gas content was used to calculate the level of supersaturation that was not allowed to exceed a maximum value by the algorithm. A decompression was considered unsafe with the inevitability of DCS if the critical supersaturation was exceeded in any compartment, or safe with no possibility of DCS if the critical supersaturation was not exceeded in any compartment. Although this approach has since been extensively refined [6-10], it retains the shortcoming of being unable to explicitly control the risk of DCS in the calculation of decompression schedules.

Recognizing that the occurrence of DCS has both deterministic and stochastic mechanisms, workers at the United States Navy (USN) Naval Medical Research Institute (NMRI) developed models to predict the probability of DCS occurrence during hyperbaric exposures and compute decompression schedules that incur user-specified risks of DCS [11-23]. These models feature calibration against data describing a collection of hyperbaric exposures and their binary outcomes: either DCS occurred or it did not. There is currently no definitive diagnostic test for DCS. In the absence of a definitive test, the outcomes of some dives are an ambiguous collection of signs and symptoms. These ambiguous outcomes are termed marginal DCS events, do not require recompression therapy, and spontaneously resolve. Examples of marginal DCS events are aches or mild pain in a single joint lasting less than 60 minutes or pain in multiple joints lasting less than 30 minutes [24, 25]. Pain with any other manifestation, such as visual disturbances, and difficulties with balance, speech, and/or comprehension, whether or not these other manifestations self-resolve, would not be classified as a marginal DCS event.

Transient or ambiguous symptoms indicate potential occurrence of the sickness. In order to incorporate marginal DCS events, these occurrences were originally treated as half of a DCS event (weighted as 0.5) when included in the calibration data [13], though no statistical justification was given for this decision. Later, the weight given to marginal events was reduced to one-tenth of a DCS event based upon communications with USN dive medical officers, who indicated they were much less concerned with marginal DCS than full DCS [19]. More rigorous methods for incorporating different degrees of severity of DCS have since been published [26]. Recent work has found the inclusion of marginal DCS events with fractional weights detrimental to the overall performance of probabilistic models [27]. Rigorous statistical evaluation of marginal events has found that they are not combinable with the rest of the data in the BIG292 calibration set used by the authors. This past study points to the fact that while saturation data makes up 14.4% of the BIG292 calibration data set (discussed in more detail below) and marginal DCS events account for 3.3% of BIG292, 55% of the marginal DCS events occurred

during saturation dives. This indicates that including marginal DCS events, even with a small fractional weight, grants saturation exposures undue weight in the calibration data. In this work, we evaluate the impact of treating marginal DCS events as non-events in the calibration data. We first determine if linear kinetics, a threshold term, and oxygen as a participating gas are still beneficial to model performance; as determined previously [12, 15, 17, 19]. After we establish which model features are statistically justified, we investigate how the modified calibration data affects model performance.

Methods

Data

All data used in this study were taken from the USN N_2-O_2 dive database which has been previously published [12, 24, 25, 28] and does not require approval from an institutional review board for use. The data are composed of time-series records for the pressure and gas inspired by the diver throughout each recorded dive. Successive points or "nodes" are connected by straight lines in the time domain to describe a dive as a series of segments, each of which is either an isobaric, compression, or decompression segment that may include a breathing gas switch. The outcome of each exposure is recorded as either 1.0 if DCS occurred, 0.0 if DCS did not occur, or 0.1 if marginal DCS occurred. If the outcome was DCS or marginal DCS, the time the subject was last known to be symptom free and the time at which the presence of DCS signs or symptoms were first confirmed are also recorded. Two subsets of the USN N_2-O_2 dive database were used in this study. The first set, BIG292, consists of 3,322 exposures in 1,038 different time and depth profiles within which 190 DCS events and 110 marginal DCS events occurred. BIG292 was used as the calibration data set for the LE1-USN93 model parameters [29]. The second set, NMRI98, augments BIG292 with an additional 1,013 exposures in 266 additional profiles. These additional exposures used gases with increased oxygen content during either or both the on-bottom and decompression (ascent) phases of the dives. The inclusion of more profiles using gases with

increased oxygen content makes the NMRI98 data set a more versatile calibration set than BIG292. The NMRI98 data set has a total of 223 full DCS events and 127 marginal DCS events. NMR98 was used as the calibration data set for a study of models incorporating oxygen as a participating gas [12, 17].

Models

The PLBX3 exponential-exponential model [30, 31], the linear-exponential model (LE1) [29], and the linear exponential multigas model (LEM) [12, 17, 32] were chosen as the basis for this work. Features of these models are summarized in Table 1. Each is a survival model in which the body is considered to consist of three independent, well-stirred, perfusion-limited gas exchange compartments. These compartments are not intended to represent distinct anatomical tissues, but are mathematical abstractions with no direct relationship to the underlying physiology. In each model, the probability of DCS for a given exposure, PDCS, is given as a function of the instantaneous risk of DCS, r_i, in each of $n=3$ compartments:

$$PDCS = 1 - e^{-\sum_i^n g_i \int r_i dt}, \tag{1}$$

where, g_i is a compartmental scaling term or gain. This equation does not include time of onset and is integrated from the start of the dive to the right-censored time, the time at which observation ceased. Time of symptom onset is incorporated by calculating a joint probability including the probability of being symptom free (PS) until the last known time at which the subject was symptom free, T_1, and the probability of DCS occurring between T_1 and T_2, the time at which the presence of symptoms was first confirmed [33]

$$PDCS = PS_{T_1} PDCS_{T_1,T_2} = e^{-\sum_i^n g_i \int_0^{T_1} r_i dt} \left(1.0 - e^{-\sum_i^n g_i \int_{T_1}^{T_2} r_i dt} \right). \tag{2}$$

In the absence of gas bubbles, the rate of change of the compartmental inert gas tension is

$$\frac{dP_T}{dt} = k(P_{N_2}^0 + R_{N_2} t) - kP_T \,, \tag{3}$$

where k is a rate constant for the compartment and P_T is the tissue tension of the dissolved inert gas (nitrogen for this document), $P_{N_2}^0$ is the nitrogen pressure at the beginning of the segment, R_{N_2} is the rate of change of the arterial inert gas tension during the dive segment, and t is time. The arterial inert gas tension is assumed to be in equilibrium with the alveolar gas. The solution to the differential Eq. (3) for the duration of a dive segment is the familiar mono-exponential expression [11, 13, 27, 34] given by

$$P_T = \alpha e^{-kt} + R_{N_2} + \beta \,, \tag{4}$$

where the constants for the dive segment are

$$\begin{aligned} \alpha &= P_T^0 - P_{N_2}^0 + \frac{R_{N_2}}{k} \\ \beta &= P_{N_2}^0 - \frac{R_{N_2}}{k} \end{aligned} \,, \tag{5}$$

and P_T^0 is the tissue tension at the beginning of the dive segment.

Both gas uptake and elimination are mono-exponential in the PLBX3 model compartments [30, 31]. Compartmental gas elimination in the LE1 and LEM models is allowed to be time linear in one compartment after a crossover compartmental tension P_{XO} is exceeded. Linear kinetics were introduced as a mechanism for modeling the reduced rate of inert gas elimination caused by the formation of gas bubbles in that compartment [29, 35]. The linear gas kinetics are defined as

$$P_T = P_T^0 + k(P_{N_2}^0 - P_B^0 - P_{XO} - P_{FVG})t + \frac{k(R_{N_2} - R_B)}{t^2} \tag{6}$$

where P_B^0 is the ambient pressure at the start of the dive segment and R_B is the rate of change in ambient pressure in the dive segment. This condition can only occur when supersaturation is present. Therefore, the tissue tension (or inert gas burden) evolves as

$$\begin{aligned} P_T &= \alpha e^{-kt} + R_{N_2} + \beta && ;P_T < P_B + P_{XO} - P_{FVG} \\ P_T &= P_T^0 + k(P_{N_2}^0 - P_B^0 - P_{XO} - P_{FVG})t + \frac{k(R_{N_2} - R_B)}{t^2} && ;P_T \geq P_B + P_{XO} - P_{FVG} \end{aligned} \quad (7)$$

where P_B is the ambient pressure and P_{FVG} is the total partial pressure of the metabolic gases; oxygen, carbon dioxide, and water vapor; presumed constant and equal to $0.1917\,\mathrm{atm}$ [36].

In all three models, the instantaneous risk for the i^{th} compartment (r_i) is given in terms of the prevailing compartmental gas supersaturation, ($P_{Ti} + P_{FVG} - P_B$):

$$r_i = \frac{P_{T_i} - P_B - Thr_i + P_{FVG}}{P_B}, \quad (8)$$

where Thr_i is a threshold supersaturation that must be exceeded before risk accumulates in the compartment. For compartments which do not have a threshold, *Thr* is set to 0.

LEM further enhances the LE1 model with the addition of oxygen as a participating gas in the compartment with linear gas kinetics. In order to include oxygen as a participating gas, the tissue tension is redefined as

$$P_T = P_{T_{N_2}} + P_{T_{O_2}} \quad (9)$$

subject to the conditions

$$\begin{aligned} P_{eff_{O_2}} &= P_{O_2} - PSET ; P_{O_2} > PSET \\ P_{eff_{O_2}} &= 0 \qquad\qquad ; P_{O_2} \leq PSET \end{aligned} \quad (10)$$

where *PSET* is a fitted parameter determining the concentration above which oxygen ceases to be treated as completely metabolized and becomes part of the inert gas burden in the tissue. $P_{eff_{O_2}}$ is the partial pressure of oxygen treated as an inert gas. Both conditions are implemented during gas uptake and elimination.

Models were optimized using likelihood maximization [11, 37, 38]. Gain variables can be calculated directly [39], but were left as fitted parameters in the present work due to the ease of programming. Likelihood is defined as the probability of the observed outcome [11, 38]. The likelihood L for each exposure i is given by

$$L_i = PDCS_i^{\delta_i}(1 - PDCS_i)^{1-\delta_i}, \tag{11}$$

where δ is the outcome, $\delta = 0$ indicates no DCS, $\delta = 1$ indicates DCS occurred, and $\delta = W_m$ for marginal events. Marginal DCS events were treated as non-events with an outcome of $W_m = 0.0$. The joint probability of all N observed outcomes can be calculated as

$$L = \prod_i^N PDCS_i^{\delta_i}(1 - PDCS_i)^{1-\delta_i}, \tag{12}$$

by assuming that the outcome of each exposure is independent of all other observed outcomes. For ease of computation, we work with the log of each likelihood value and negate the final sum to phrase the problem as a maximization. We used the Nelder-Mead maximization algorithm [40], which is gradient-free and robust, to avoid numerical difficulties arising from discontinuities in the parameter space [34]. 32 solutions were obtained for each model tested; starting from different initial values of the free parameters. The best (maximum log likelihood) parameter set was selected for each model for model comparison. The LE1 and PLBX3 models were fit to the BIG292 data set for comparison with the LE1-USN93 model and parameter set. All other models tested were fit to the NMRI98 data.

Model Selection

The LEM model is produced by the progressive addition of linear kinetics, a threshold term, and oxygen to the most reduced model, PLBX3. All models tested were consequently nested within the least reduced LEM model. The statistical justification for addition of each added model feature was tested with MATLAB (MathWorks MATLAB 2015b) log likelihood difference tests with a significance level of 0.05 as the selection criterion and with the Akaike Information Criterion (AICc) [41] defined in Eq. (13). In Eq. (13), *K* is the number of free parameters and N is the sample size.

$$AICc = -2(\ln(likelihood)) + 2K\left(\frac{N}{N-K-1}\right) \tag{13}$$

The weighted AIC index, defined in Eq. (14), provides an easier-to-interpret statistic in which each model is assigned a number between 0.0 and 1.0. The model with value closest to 1.0 is the model that best describes the data.

$$weightedAICIndex = \frac{e^{-0.5\Delta AICc}}{\sum_{i=1}^{m} e^{-0.5\Delta AICc_i}} \tag{14}$$

Calculation of No-Stop Limits

The no-stop limit for a given dive depth is the maximum time that can be spent at that depth and followed by a direct ascent to surface while producing a risk of DCS that reaches but does not exceed a pre-specified limit. No-stop limit prescriptions of the present models optimized with marginal DCS events weighted as 0.1 and 0.0 were compared to limits in the USN Diving Manual Revision 7 (VVAL-79 Thalmann Algorithm [6, 42, 43]) and to limits prescribed by the LE1-USN93 and LEM-NMRI98 models. The no-stop limits were calculated assuming air breathing throughout each exposure with descent and ascent rates of 75 fpm and 30 fpm, respectively [44]. Descent time was not included in the bottom time. A 2.3% acceptable risk of DCS was used to be consistent with prior USN work [22]. Starting with a bottom time

of one minute, the no-stop limit at each dive depth was determined by incrementing the bottom time in one minute intervals until the 2.3% risk level was reached.

Results and Discussion

Deleting the weight of marginal events (W_m = 0.0) for model calibration against BIG292 resulted in LE1 remaining the best selected model. After reparameterization with W_m = 0.0 we compared LE1 against the less complex PLBX3 model and found that the additional complexity was justified with a p-value of 5.61E-06 by the log likelihood difference test. The weighted AICc index for LE1 was 0.99, indicating that LE1 provided a much better description of BIG292 than PLBX3. Best-fit parameters along with their 95% confidence intervals for both models are provided in Table 2. The confirmation that LE1 remains the best descriptor of BIG292 is unsurprising. Weighting marginal events as non-events (W_m = 0.0) within the training set does not change the dive profiles. Since all dive types (single air, single non-air, saturation, *et cetera*) are still present, all modifications which enhance the three independent, well-stirred, and perfusion-limited compartment class of models are still necessary.

Figure 1 graphs the probability of DCS for each profile predicted by the LE1-USN93 model (W_m = 0.1) versus the probabilities predicted by LE1 with refit parameters (W_m = 0.0). The predicted probabilities were sorted from smallest to largest to more easily observe trends. The performance of the LE1 model on saturation exposures is not significantly altered by reducing W_m to 0.0, despite marginal events predominantly occurring during saturation exposures. In Figure 2, the predicted probabilities of all non-saturation exposures from BIG292 are plotted; again after sorting the probabilities from smallest to largest. The PDCS predictions from the parameters optimized with W_m = 0.0 are the abscissa and the predictions from LE1-USN93 (W_m = 0.1) are the ordinate. The PDCS predictions from the refit parameters with W_m equal to 0.0 are consistently lower than the PDCS predictions of LE1-USN93 (W_m = 0.1). From this we conclude that the bulk of the risk resulting from marginal DCS events is spread across the non-

211 saturation profiles, despite being predominantly associated with the saturation dives. This agrees with
212 our previous finding [27] that marginal DCS events weighted as W_m = 0.1 degrade model performance for
213 non-saturation dives. As shown in Figure 3 there is no significant change in the distribution of which
214 compartments contribute to the overall risk.

215 Occurrence density functions (ODFs) plot the number of DCS occurrences per hour centered on
216 the time of surfacing from the dive. Negative time values indicate DCS occurred prior to the diver
217 surfacing. Figure 4 shows the ODF for BIG292 along with the ODFs for the LE1-USN93 (W_m = 0.1)
218 parameters and our refit parameters for the LE1 model (W_m = 0.0). The true values from the BIG292 data
219 contain a bimodal peak near the time of surfacing. Neither version of LE1 reproduces this behavior and
220 the source of the bimodal peak. In our recent investigation into the source of the bimodality for the dive
221 trial data, we found that the bimodality was most likely caused by a change in DCS onset time reporting
222 protocol in 1984 and was not related to dive type or DCS event severity [45]. The reduction in value of
223 W_m from 0.1 to 0.0 results in a smaller peak near the time of surfacing, but does not significantly change
224 the shape or position of the peak.

225 For the larger NMRI98 data set, we tested all combinations of model enhancements nested within
226 the LEM model optimized with W_m assigned a value of 0.0. Optimization and test results for each of the
227 models are given in Table 3. LEM was the best descriptor of these data with a weighted AICc index of
228 0.97. It also performed the best by the log likelihood difference test. The best fit model parameters and
229 their 95% confidence intervals are given in Table 4. The best fit value of *PSET* in Model 5 was 25.9 atm, a
230 value which is far in excess of the highest oxygen partial pressure encountered in any dive in the training
231 data, and indeed of any oxygen partial pressure allowed during actual dive operations [46]. Thus, the
232 potential to use oxygen as a participating gas in Model 5 was not exercised and the model collapsed into
233 Model 3.

Plotting the change in predicted probability of DCS for the LEM model optimized with the NMRI98 data as depicted in Figure 5 shows that unlike the LE1 model, reducing the value of W_m from 0.1 to 0.0 reduces the risks of saturation dives. The same saturation dive subsets; ASATARE, ASATEDU, ASATNMR, and ASATNSM described by Temple et al [24, 25]; are contained in both BIG292 and NMRI98. Unlike LE1, LEM did not predict higher probabilities of DCS for non-saturation dives when marginal DCS events are weighted as 0.1. The predicted number of full DCS cases for the saturation dives with W_m = 0.1 is 59.39 and the predicted number of cases with W_m = 0.0 is 52.94 while the actual number is 52. Thus, interpreting marginals as no DCS yields a LEM model that does a better job of predicting the actual number of cases. Figure 6 shows that only a small number of non-saturation dives had their risks significantly lowered by the reduction of W_m from 0.1 to 0.0; most non-saturation exposures had very little change. The risk contributions from each compartment normalized by the total risk are plotted in Figure 7. Each compartment's risk contribution did shift, but there were no significant qualitative changes. For the models optimized with and without marginal DCS events given fractional weight, the majority of the dives in the data set accumulate risk in at most two compartments. This may be inferred from the fact that the majority of the points fall on or close to the outer boundaries of the plot. If an exposure accumulated risk in all three compartments, then that point would fall closer to the center of the plot. The clustering of points on or close to the outer boundaries shows that exposures tend to accumulate risk either in the fast and intermediate compartments or in the intermediate and slow compartments.

The ODF for the NMRI98 data is qualitatively the same as that of the BIG292 data, at least partly because NMRI98 is a superset of BIG292. Weighting marginal DCS events as non-events (W_m = 0.0) in the LEM model's training set did not significantly impact the large peak centered at the time of surfacing as is evident in Figure 8. This is consistent with non-saturation dives being relatively unchanged by the classification of marginals as non-events. DCS associated with non-saturation dives typically occurs within two hours after reaching the surface, whereas during saturation dives DCS is not uncommon during the

ascent phase of the dive [24, 25]. Reducing W_m to 0.0 results principally in a reduction of the small numbers of events in the tail of the distribution associated with DCS occurrences before the divers surfaced.

The air diving no-stop limits prescribed by our LE1 and LEM models fit to their respective training datasets with W_m = 0.0 are compared to the current USN guidance [44] in Table 5. The LE1 prescriptions are consistently longer than those of LE1-USN93 (W_m = 0.1), which is expected since decreasing W_m to 0.0 reduces the bulk probability of DCS by reducing the number of DCS events in the training data. LEM prescriptions for dives to shallow depths (70 fsw and less) are shorter than the corresponding air no-stop limits, while the prescriptions for dives to greater depths are consistently longer. In Figure 9, we plot our new no-stop prescriptions along with the VVal-79 Thalmann algorithm prescriptions. As depicted in the graph, there is good agreement between all three algorithms except for shallow depths. Four of the proposed no-stop limits have been man-tested in previous work [47, 48]: 20 minutes at 130 FSW, 15 minutes at 150 FSW, 12 minutes at 150 FSW, and 9 minutes at 190 FSW. The rate of DCS occurrence in these trials was less than 2.3%, but there was an unacceptably high number of Type 2 DCS events.

Conclusions

Models for estimating the probabilities of DCS in diving have conventionally considered the occurrence of DCS to be a binary event with an outcome weighting of unity if it occurs or a weighting of zero if it does not occur in a given dive. Desire to include information for dives in which the DCS outcome is not clear has motivated consideration of such outcomes as marginal DCS events with *ad-hoc* fractional weighting. Previous work has shown that they should be treated as non-events with weights of W_m = 0.0 for model optimization [27]. LE1 and LEM remained the best descriptors of BIG292 and NMRI98, respectively, after their parameters were reoptimized with W_m = 0.0. The risk distributions for each of the refit models were affected very differently by reducing W_m from 0.1 to 0.0. LE1 placed the bulk of the

281 risk associated with marginal weights of $W_m = 0.1$ on the non-saturation dives despite a disproportionately
282 large portion of marginal DCS events occurring during saturation dives. In contrast, LEM correctly placed
283 the bulk of the risk associated with marginal weights of $W_m = 0.1$ on the saturation dives indicating that it
284 is a better descriptor of the NMRI98 data set.

285 The models refit with $W_m = 0.0$ prescribed no-stop limits for air diving similar to those published
286 in the USN Dive Manual Revision 7 [46]. No-stop limits prescribed by the LE1 model were consistently
287 longer, consistent with the ascription of less risk to the non-saturation dives. The LEM model had small
288 adjustments to its no-stop prescriptions. The close agreement of all three algorithms' prescriptions
289 provide further evidence that W_m should equal 0.0 when optimizing models for predicting the occurrence
290 of DCS. The confirmation of $W_m = 0.0$ indicates that the information contained in marginal DCS events
291 must be incorporated by an entirely different mechanism than what has been used thus far. We propose
292 that treating marginal DCS events as a different type of severity instead of a weighted binary outcome is
293 a more appropriate way of incorporating the information from these events. This can be accomplished
294 using existing techniques for incorporating severity information [26] as no DCS, marginal DCS, and full DCS
295 instead of differentiating by type 1 and type 2; or by extending existing techniques to include four
296 severities: no DCS, marginal DCS, type 1, and type 2. Finally, it is worth pointing out that probabilistic DCS
297 models are inexact and the conclusions drawn in this paper might be dependent upon the probabilistic
298 models used for this study.

299 Acknowledgement

300 This work was supported by Naval Sea Systems Command (NAVSEA-00C - http://www.navsea.navy.mil/)
301 under contract #N00024-13-C-4104 and the Office of Naval Research under grant N000141310063.
302 BelleQuant Engineering, PLLC provided computational resources. Neither the funding agency nor the
303 commercial entity played any role in designing this study, data collection and analysis, decision to
304 publish, interpreting the results, or writing the manuscript.

Bibliography

[1] A.A. Bove, Bove and Davis' diving medicine, WB Saunders Philadelphia2004.
[2] T.J.R. Francis, S.J. Mitchell, Pathophysiology of decompression sickness, Bennett and Elliott's physiology and medicine of diving. 5th ed. London: Saunders, (2003) 530-556.
[3] R.D. Vann, F.K. Butler, S.J. Mitchell, R.E. Moon, Decompression illness, Lancet, 377 (2011) 153-164.
[4] R.D. Vann, P.J. Denoble, L.E. Howle, P.W. Weber, J.J. Freiberger, C.F. Pieper, Resolution and severity in decompression illness, Aviation, Space, and Environmental Medicine, 80 (2009) 466-471.
[5] A.E. Boycott, G. Damant, J.S. Haldane, The prevention of compressed-air illness, Journal of Hygiene, 8 (1908) 342-443.
[6] E.D. Thalmann, Phase II testing of decompression algorithms for use in the U.S. Navy underwater decompression computer, U.S. Navy, NEDU Report 1-84, 1984
[7] E.D. Thalmann, Testing of decompression algorithms for use in the US Navy underwater decompression computer, U.S. Navy, NEDU Report 11-80, 1984
[8] R.D. Workman, Calculation of air saturation decompression tables, U.S. Navy, NEDU Report 11-17, 1957
[9] R.D. Workman, Calculation of decompression schedules for nitrogen-oxygen and helium-oxygen dives, U.S. Navy, NEDU Report 6-65, 1965
[10] A.A. Bühlmann, Decompression—Decompression Sickness, Springer Science & Business Media1984.
[11] P.K. Weathersby, L.D. Homer, E.T. Flynn, On the likelihood of decompression sickness, Journal of Applied Physiology, 57 (1984) 815-825.
[12] E.C. Parker, S.S. Survanshi, P.B. Massell, P.K. Weathersby, Probabilistic models of the role of oxygen in human decompression sickness, Journal of Applied Physiology, 84 (1998) 1096-1102.
[13] P.K. Weathersby, S.S. Survanshi, L.D. Homer, B.L. Hart, R.Y. Nishi, E.T. Flynn, M.E. Bradley, Statistically based decompression tables I: Analysis of standard air dives: 1950-1970, U.S. Navy, NMRI Report 85-16, 1985
[14] P.K. Weathersby, J.R. Hays, S.S. Survanshi, L.D. Homer, B.L. Hart, E.T. Flynn, M.E. Bradley, Statistically based decompression tables II: Equal risk air diving decompression schedules, U.S. Navy, NMRI Report 85-17, 1985
[15] P.K. Weathersby, S.S. Survanshi, J.R. Hays, M.E. MacCallum, Statistically based decompression tables III: Comparitive risk using U.S. Navy, British, and Canadian standard air schedules, U.S. Navy, NMRI Report 86-50, 1986
[16] J.R. Hays, B.L. Hart, P.K. Weathersby, S.S. Survanshi, L.D. Homer, E.T. Flynn, Statistically based decompression Tables IV: Extension to air and N2-O2 saturation decompression, U.S. Navy, NMRI Report 86-51, 1986
[17] E. Parker, S. Survanshi, E. Thalmann, P. Weathersby, Statistically Based Decompression Tables IX: Probabilistic Models of the Role of Oxygen in Human Decompression Sickness, U.S. Navy, NMRI Report 96-05, 1996
[18] Y.J. Parsons, P.K. Weathersby, S.S. Survanshi, E.T. Flynn, Statistically based decompression tables V: Haldine-Vann models for air diving, U.S. Navy, NMRI Report 89-34, 1989
[19] E.C. Parker, S.S. Survanshi, P.K. Weathersby, E.D. Thalmann, Statistically based decompression tables VIII: Linear-exponential kinetics, U.S. Navy, NMRI Report 92-73, 1992
[20] S. Survanshi, P. Weathersby, E. Thalmann, Statistically based decompression tables X: Real-time decompression algorithm using a probabilistic model, U.S. Navy, NMRI Report 96-06, 1996
[21] P.K. Weathersby, S.S. Survanshi, R.Y. Nishi, E.D. Thalmann, Statistically dased decompression tables VII: Selection and treatment of primary air and N2O2 data, U.S. Navy, Joint Report NSMRL Report 1192 and NMRI Report 92-85, 1992

[22] S.S. Survanshi, E.C. Parker, E.D. Thalmann, P.K. Weathersby, Statistically based decompression tables XII: Volume I. Repetitive decompression tables for air and constant 0.7 ATA PO2 in N2 using a probabilistic model, U.S. Navy, NMRI Report 97-36, 1997
[23] G.W. Albin, P.K. Weathersby, Statistically based decompression tables VI. Repeat Dives on Oxyen/Nitrogen Mixes, N. U.S., NMRI Report 91-84, 1991
[24] D.J. Temple, R. Ball, P.K. Weathersby, E.C. Parker, S.S. Survanshi, The dive profiles and manifestations of decompression sickness cases after air and nitrogen-oxygen dives. Volume I: Data set summaries, manifestation descriptions, and key files, U.S. Navy, NMRC Report 99-02 (Vol. I), 1999
[25] D.J. Temple, R. Ball, P.K. Weathersby, E.C. Parker, S.S. Survanshi, The dive profiles and manifestations of decompression sickness cases after air and nitrogen-oxygen dives. Volume II: Complete profiles and graphic representations for DCS events, U.S. Navy, NMRC Report 99-02 (Vol. II), 1999
[26] L.E. Howle, P.W. Weber, E.A. Hada, R.D. Vann, P.J. Denoble, The probability and severity of decompression sickness, PLoS ONE, 12 (2017) e0172665.
[27] L.E. Howle, P.W. Weber, R.D. Vann, M.C. Campbell, Marginal DCS events: Their relation to decompression and use in DCS models, Journal of Applied Physiology, 107 (2009) 1539-1547.
[28] D.J. Doolette, W.A. Gerth, K.A. Gault, Addition of work rate and temperature information to the augmented NMRI standard (ANS) data files in the "NMRI98" subset of the USN N_2–O_2 primary data set, U.S. Navy, NEDU Report 11-02, 2011
[29] E.D. Thalmann, E.C. Parker, S.S. Survanshi, P.K. Weathersby, Improved probabilistic decompression model risk predictions using linear-exponential kinetics, Undersea & Hyperbaric Medicine, 24 (1997) 255-274.
[30] F.G. Murphy, E.A. Hada, D.J. Doolette, L.E. Howle, Probabilistic pharmacokinetic models of decompression sickness in humans part 1: Coupled perfusion-limited compartments, Computers in Biology and Medicine, 86 (2017) 55-64.
[31] F.G. Murphy, The impact of weighting marginal DCS events as non-events, pharmacokinetic gas content models, and optimal decompression schedule calculation (Doctoral Dissertation), Mechanical Engineering and Materials Science Department, Duke University, Durham, NC, 2017, pp. 194.
[32] W.A. Gerth, T.M. Johnson, 1.3 ATA PO2-in-He decompression tables for MK 16 MOD 1 UBA, U.S. Navy, NEDU Report 02-10, 2002
[33] P.K. Weathersby, S.S. Survanshi, L.D. Homer, E.C. Parker, E.D. Thalmann, Predicting the time of occurrence of decompression sickness, Journal of Applied Physiology, 72 (1992) 1541-1548.
[34] L.E. Howle, P.W. Weber, R.D. Vann, A computationally advantageous system for fitting probabilistic decompression models to emperical data., Computers in Biology and Medicine, 39 (2009) 1117 - 1129.
[35] R.S. Srinivasan, W.A. Gerth, Mathematical models of diffusion-limited gas bubble evolution in perfused tissue, U.S. Navy, NEDU Report 13-05, 2013
[36] W.A. Gerth, R.D. Vann, Probabilistic gas and bubble dynamics models of decompression sickness occurrence in air and nitrogen-oxygen diving., Undersea & Hyperbaric Medicine, 24 (1997) 275-292.
[37] R.A. Fisher, On the mathematical foundations of theoretical statistics, Philosophical Transactions of the Royal Society London A, 222 (1921) 309-368.
[38] W.A. Gerth, Overview of survival functions and methodology, in: P.K. Weathersby, W.A. Gerth (Eds.) Fifty-first Workshop of the Undersea and Hyperbaric Medical SocietySeattle, WA, 2002, pp. 1-48.
[39] L.E. Howle, Analytic gain in probabilistic decompression sickness models, Computers in Biology and Medicine, 43 (2013) 1739-1747.
[40] J. Nocedal, S. Wright, Numerical Optimization, Springer Science & Business Media 2006.
[41] K.P. Burnham, D.R. Anderson, Model Selection and Multimodel Inference: A Practical Information-Theoretic Approach, Springer Science & Business Media 2002.

399 [42] W.A. Gerth, D.J. Doolette, VVal-79 maximum permissible tissue tension table for Thalmann
400 algorithm support of air diving, U.S. Navy, NEDU Report 12-01, 2012
401 [43] W.A. Gerth, D.J. Doolette, VVal-79 Thalmann algorithm metric and imperial air decompression
402 tables, U.S. Navy, NEDU Report 16-05, 2016
403 [44] N.S.S.C. Commander, U.S. Navy Diving Manual, Revision 6, U.S. Navy, 2008
404 [45] A.E. King, F.G. Murphy, L.E. Howle, Bimodal decompression sickness onset times are not related to
405 dive type or event severity, Computers in Biology and Medicine, 91 (2017) 59-68.
406 [46] N.S.S.C. Commander, U.S. Navy Diving Manual, Revision 7, U.S. Navy, 2017
407 [47] D.J. Doolette, W.A. Gerth, K.A. Gault, Empirical evaluation of extensions to no-stop limits for deep
408 air giving, Undersea & Hyperbaric Medicine, 34 (2007) 232.
409 [48] D.J. Doolette, W.A. Gerth, K.A. Gault, Risk of central nervous system decompression sickness in air
410 diving to no-stop limits, U.S. Navy, NEDU Report 09-03, 2009

411

412

Model	Linear Kinetics	Oxygen	Threshold
PLBX3			
Model 1	X		
Model 2		X	
Model 3			X
LE1 (USN93)	X		X
Model 4	X	X	
Model 5		X	X
LEM (LEM-NMRI98)	X	X	X

Table 1: Summary of features in the models investigated. All models are composed of three parallel, uncoupled, well-stirred compartments. Exponential gas uptake and elimination prevailed in each compartment unless otherwise noted by an "X" in the Linear Kinetics column. For the models which allowed linear gas kinetics, they were only allowed in the second compartment. Oxygen only participated in the second compartment when present. The threshold term was only applied to the third compartment.

Parameter value (+/- 95% CI)	PLBX3	LE1
g_1	3.06E-03 (3.48E-03)	3.69E-03 (4.77E-03)
g_2	4.82E-04 (3.42E-04)	8.27E-05 (4.70E-05)
g_3	2.46E-04 (3.28E-04)	1.12E-03 (2.88E-04)
k_1	5.58E-01 (3.88E-01)	6.51E-01 (5.58E-01)
k_2	4.48E-03 (1.39E-03)	1.78E-02 (8.59E-01)
k_3	2.03E-03 (1.07E-03)	1.92E-03 (2.44E-04)
PXO_2	N/A	5.57E-02 (3.01E-02)
THR_3	N/A	1.13E-01 (3.83E-02)

Table 2: Best-fit parameters with $W_m = 0.0$ for the BIG292 data. Gains are represented by g, tissue rates by k, crossover pressure to linear kinetics by PXO, and threshold for risk accumulation as THR. Subscripts indicate the compartment index to which the parameter corresponds. The 95% confidence intervals are displayed parenthetically below each parameter value.

Model	Log Likelihood	Bulk PDCS	Log Likelihood Difference	P-value	Weighted AICc
PLBX3	-1168.06	223.23	Rejected	3.79E-06	1.26E-05
Model 1	-1165.93	223.3	Rejected	8.25E-06	3.86E-05
Model 2	-1165.86	224	Rejected	2.10E-06	1.53E-05
Model 3	-1160.48	218.74	Rejected	1.50E-03	8.98E-03
LE1	-1159.14	223.39	Rejected	1.7E-03	1.26E-02
Model 4	-1167.25	223.8	Rejected	7.52E-08	1.39E-06
Model 5	-1159.47	213.08	Rejected	2.56E-04	3.33E-03
LEM	-1152.78	223.24	Accepted	N/A	9.75E-01

Table 3: Model optimization and selection results from the NMRI98 data set with $W_m = 0.0$. Bulk PDCS is the total number of cases of DCS that each model predicts for the NMRI98 data set. The observed number of DCS events was 223. Log likelihood difference testing found that the LEM model was statistically justified as the best choice with 95% certainty as the selection criterion. The actual P-values from each log likelihood difference test comparing the model to LEM are provided above. Weighted AICc index values with a closer value to 1.0 indicate better agreement with the data. The weighted AICc values do not sum to 1.0 because of rounding error.

Parameter value (+/- 95% CI)	PLBX3	Model 1	Model 2	Model 3	LE1	Model 4	Model 5	LEM
g_1	7.82E-05 (1.01E-04)	3.41E-03 (6.40E-03)	3.46E-03 (4.78E-03)	2.09E-03 (2.30E-03)	3.05E-03 (4.28E-03)	3.41E-03 (4.90E-03)	2.33E-03	3.00E-03 (3.56E-03)
g_2	6.88E-04 (1.07E-04)	7.04E-04 (6.58E-04)	3.13E-04 (7.33E-04)	6.43E-04 (9.70E-05)	6.80E-04 (1.01E-04)	1.75E-05 (2.20E-05)	4.86E-04	1.57E-04 (7.60E-05)
g_3	7.12E-03 (9.39E-03)	6.25E-02 (6.85E-04)	4.03E-04 (5.15E-01)	8.13E-03 (5.27E-03)	6.68E-03 (6.53E-03)	6.88E-04 (1.07E-04)	7.46E-04	8.63E-04 (2.94E-04)
k_1	2.55E-02 (2.32E-02)	6.44E-01 (4.91E-01)	6.44E-01 (4.53E-03)	5.03E-01 (3.93E-01)	5.91E-01 (5.08E-01)	6.43E-01 (5.31E-01)	4.34E-01	5.97E-01 (4.18E-07)
k_2	3.08E-03 (3.37E-04)	3.35E-03 (2.35E-03)	5.15E-03 (4.53E-03)	3.37E-03 (1.84E-04)	3.35E-03 (1.77E-04)	8.16E-02 (9.41E-02)	4.27E-03	1.02E-02 (2.89E-03)
k_3	1.02E-00 (5.91E-04)	5.54E-03 (2.67E-03)	2.46E-03 (1.64E-03)	1.28E-03 (1.25E-04)	2.78E-03 (9.50E-04)	3.10E-03 (3.60E-04)	1.75E-03	1.95E-03 (2.69E-04)
o_2	N/A	N/A	5.29E-02 (8.20E-02)	N/A	N/A	5.11E-02 (1.90E-01)	2.15E-02	2.86E-02 (1.22E-02)
$PSET_2$	N/A	N/A	9.44E-01 (8.20E-02)	N/A	N/A	1.05E+00 (2.01E-00)	2.59E+01	8.46E-01 (3.80E-01)
PXO_2	N/A	1.08E+04 (8.65E+00)	N/A	N/A	5.85E-01 (9.94E-02)	2.25E-02 (8.91E-02)	N/A	1.07E-01 (3.32E-02)
THR_3	N/A	N/A	N/A	5.25E-01 (5.44E-02)	4.61E-01 (4.98E-01)	N/A	1.34E-01	9.71E-02 (3.32E-02)

Table 4: Best-fit model parameters against the NMRI98 data set with marginal DCS events weighted as 0.0. Gains are represented by g, tissue rates by k, crossover pressure to linear kinetics by PXO, and threshold for risk accumulation as THR. Subscripts indicate to which compartment each parameter belongs. The 95% confidence intervals are listed below each parameter in parenthesis. The parameters used for PLBX3 have been previously reported elsewhere [30, 31].

Model	USDM, R7	LEM-NMRI98	LEM	Difference in No-Stop Times	LE1-USN93	LE1	Difference in No-Stop Times
Data Set	N/A	NMRI98	NMRI98		BIG292	BIG292	
Marginals	N/A	$W_m = 0.1$	$W_m = 0.0$		$W_m = 0.1$	$W_m = 0.0$	
30	371	234	214	-20	218	265	47
35	232	178	161	-17	163	203	40
40	163	140	128	-12	127	160	33
45	125	113	105	-8	102	129	27
50	92	94	88	-6	84	105	21
55	74	79	76	-3	71	87	16
60	63	68	66	-2	61	73	12
65	--	59	59	0	53	62	9
70	48	52	52	0	47	53	6
75	--	46	47	1	42	47	5
80	39	41	43	2	37	42	5
85	--	37	39	2	34	37	3
90	33	34	36	2	31	34	3
95	--	31	33	2	28	31	3
100	25	29	31	2	26	28	2
105	--	27	29	2	24	26	2
110	20	25	27	2	22	24	2
115	--	23	24	1	20	22	2
120	15	21	23	2	19	21	2
125	--	20	21	1	18	20	2
130	12	18	20	2	16	18	2
135	--	17	18	1	15	17	2
140	10	16	17	1	14	16	2
145	--	15	16	1	14	15	1
150	8	14	15	1	13	14	1
155	--	13	14	1	12	13	1
160	7	12	13	1	11	13	2
165	--	11	12	1	11	12	1
170	6	11	12	1	10	11	1
175	--	10	11	1	9	10	1
180	6	9	10	1	9	10	1
185	--	9	10	1	8	9	1
190	5	8	9	1	8	9	1

Table 5: Comparison of the no-stop limits prescribed for air dives by each model studied. The prescriptions from the U.S. Navy Diving Manual Revision 7 are provided for reference [46]. The left most column is depth in feet of sea water (fsw). No-stop times are calculated with a 2.3% target risk of DCS assuming a 75 fpm descent rate and 30 fpm ascent rate. Descent and ascent time is not included in the bottom time.

Bottom times are only allowed to increase in one-minute increments with the largest time not resulting in a risk higher than 2.3% being accepted as the provisionally recommended no stop time.

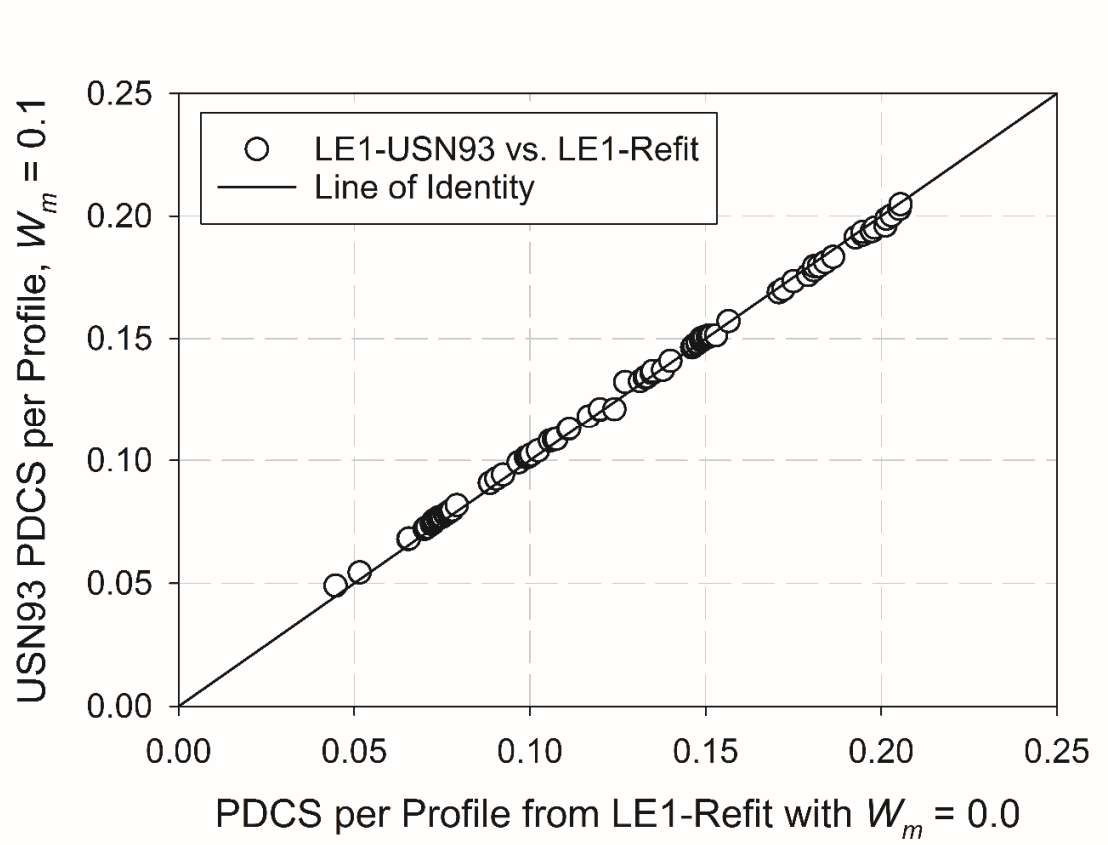

Figure 1: Shift of risk in saturation dives from the BIG292 data set. The risk of DCS was predicted for each saturation dive in the BIG292 data set. After sorting the risks from smallest to largest they were plotted with the risk predicted by our refit parameters for LE1 (derated marginal events) as the abscissa and the USN93 parameters as the ordinate.

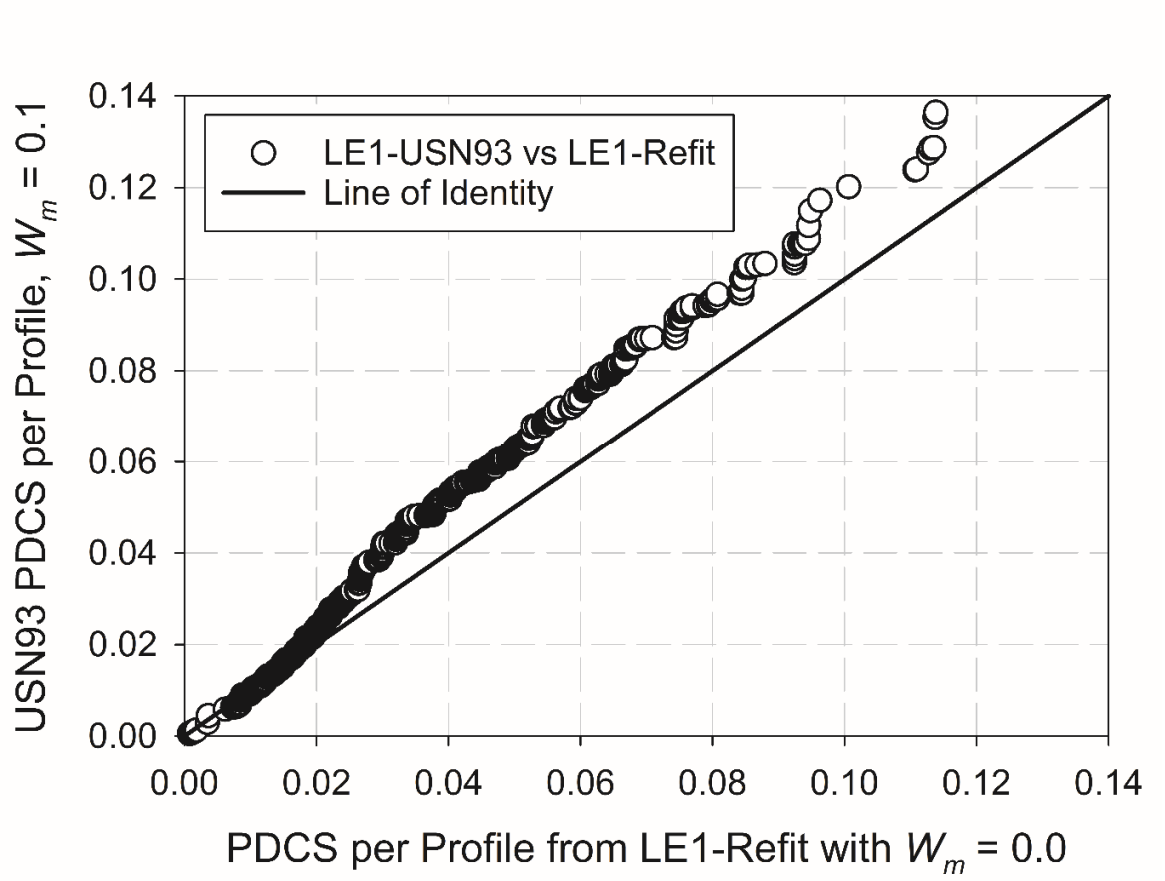

454

455 Figure 2: The risk shifts all non-saturation profiles in BIG292. The predicted risks of DCS occurring for each
456 profile are sorted from smallest to largest and plotted with the predictions from the USN93 parameters
457 as the ordinate and the predictions from our parameters optimized with derated marginal events as the
458 abscissa. Risk predictions from the parameters without marginal events in the training set are often much
459 lower than the predictions of the USN93 parameters.

460

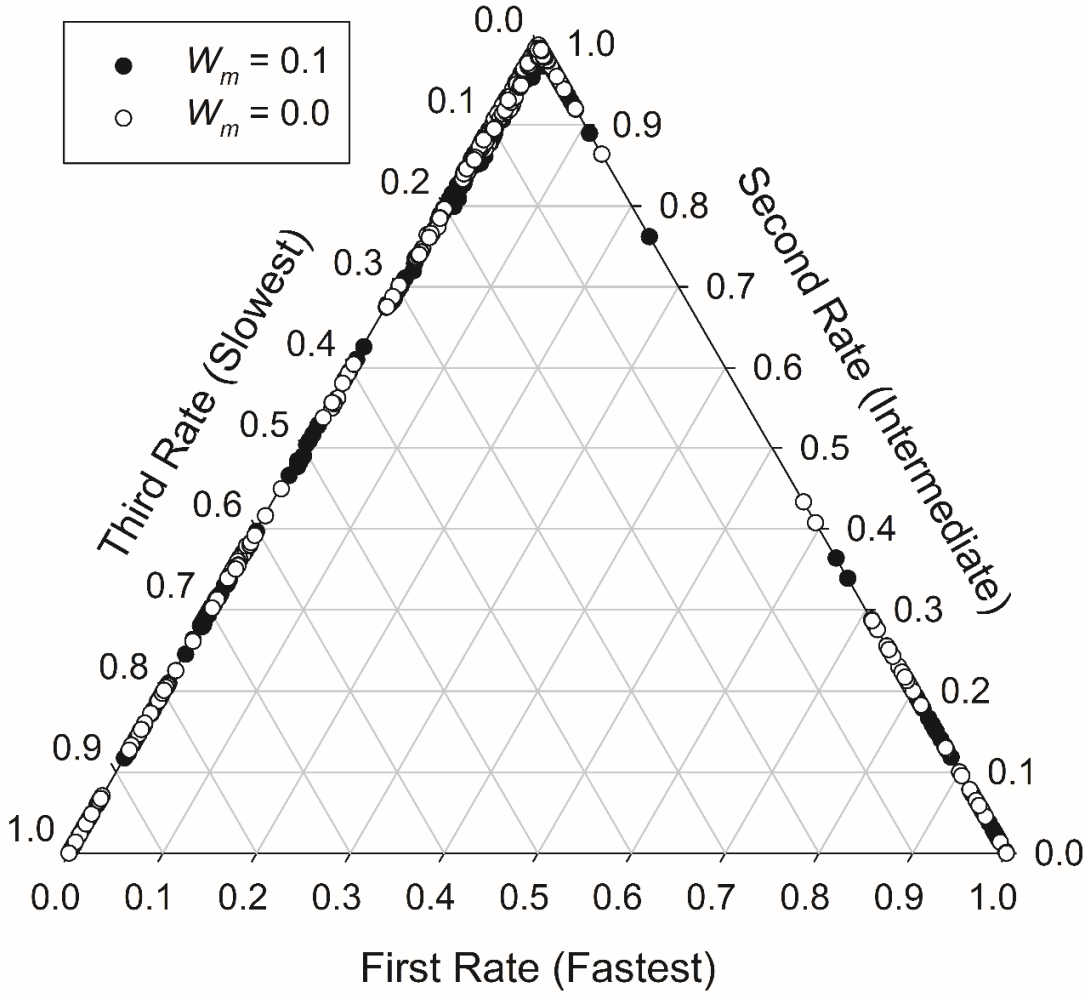

Figure 3: Ternary plot of integrated risks from all profiles in BIG292 as predicted by the LE1 model after optimization with marginal events weighted (W_m = 0.1) and with marginal events unweighted (W_m = 0.0) in the training set. Integrated risks for each compartment are normalized by the total integrated risk for the profile. The profile is then plotted on the ternary plot in which each corner represents the situation where all risk came for the compartment whose axis indicates 1.0 in the corner. As each isocline is crossed moving away from a corner the amount of risk contributed by the compartment the 1.0 belongs to decreases by 10%. While profile risks shifted positions, there was no discernable qualitative change in the overall distribution of profile risks.

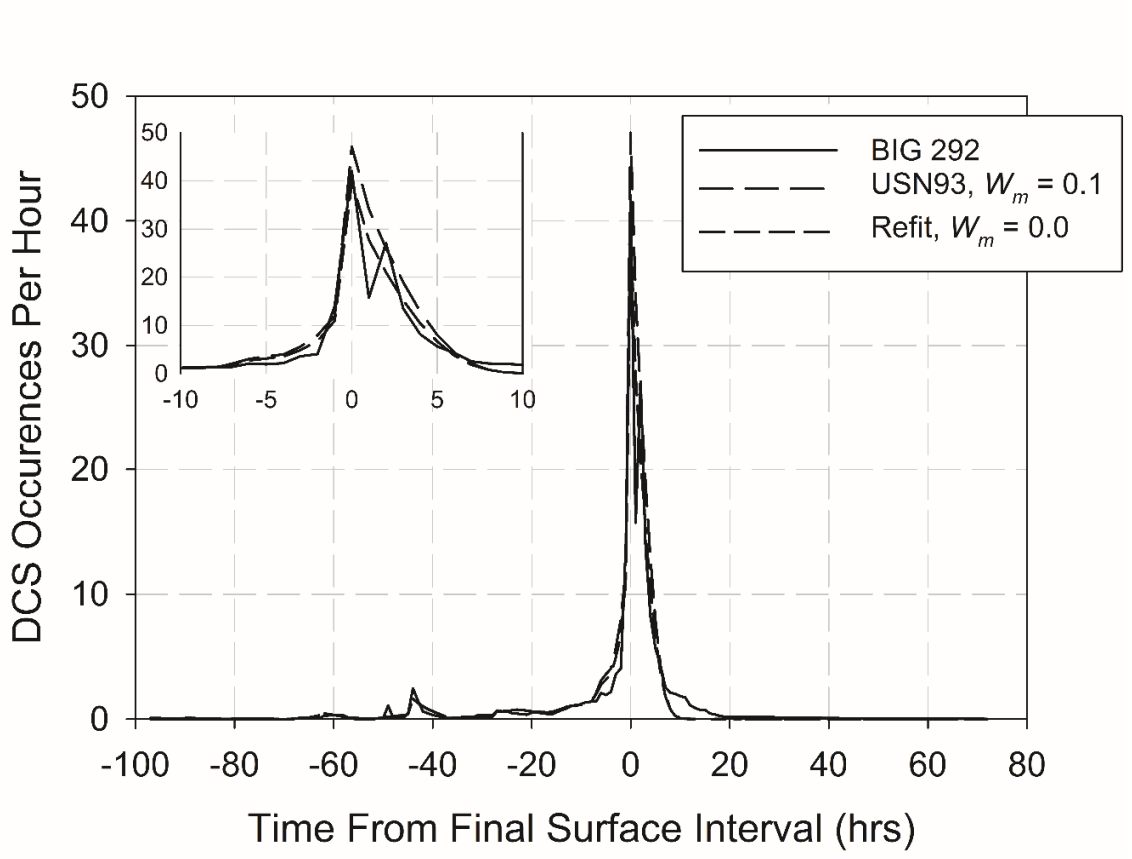

Figure 4: The occurrence density function (ODF) for the BIG292 data set. The occurrence density function plots the number of DCS events that either occurred (for the true data) or were expected (model predicted) per hour. The function is centered on the time of surfacing with negative times indicating that DCS occurred prior to the diver reaching the surface. A zoomed in view of the center of the graph is provided in the top left due to this being where the bulk of the DCS events occur. In the true data, there is a bimodal peak which is not replicated by either of the models. As expected, the number of occurrences per hour is decreased in the absence of marginal DCS events.

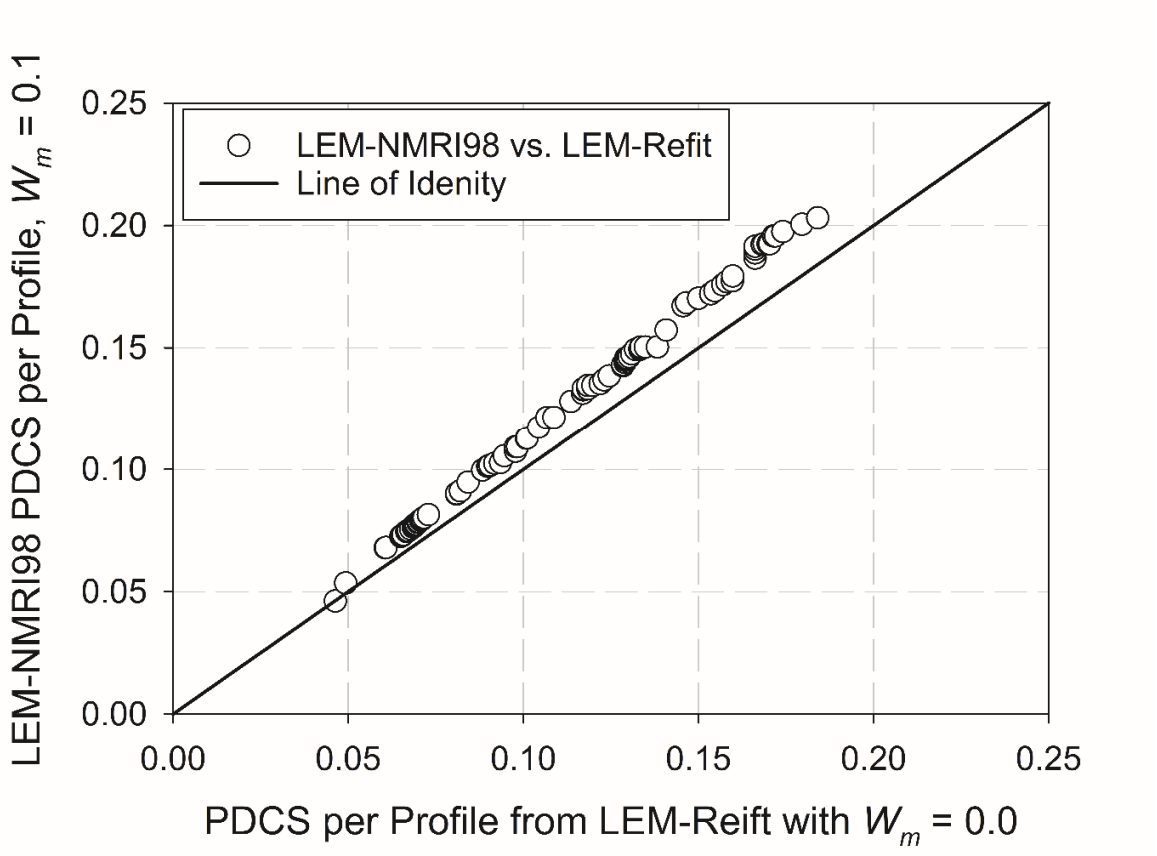

480

481 Figure 5: Shift in risk of the saturation dives in the NMRI98 data set. The risk of DCS was predicted for
482 each saturation dive in the NMRI98 data set. After sorting the risks from smallest to largest they were
483 plotted with the risk predicted by our refit parameters for LEM (W_m = 0.0) as the abscissa and the LEM-
484 NMRI98 (W_m = 0.1) parameters as the ordinate.

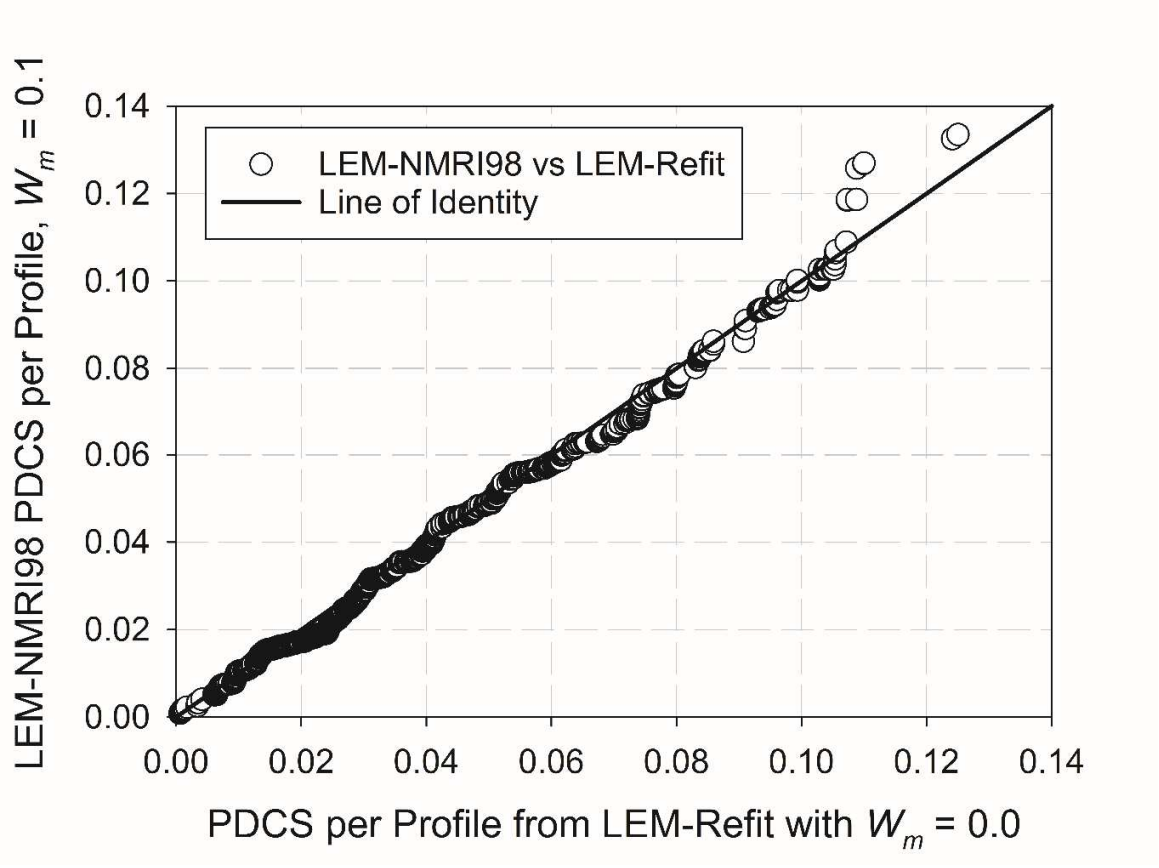

485

486 Figure 6: The risk shifts all non-saturation profiles in NMRI98. The predicted risk of DCS occurring for each
487 profile was sorted from smallest to largest and plotted with the predictions from the LEM-NMRI98 (W_m =
488 0.1) parameters as the ordinate and the predictions from our parameters optimized with W_m = 0.0 as the
489 abscissa.

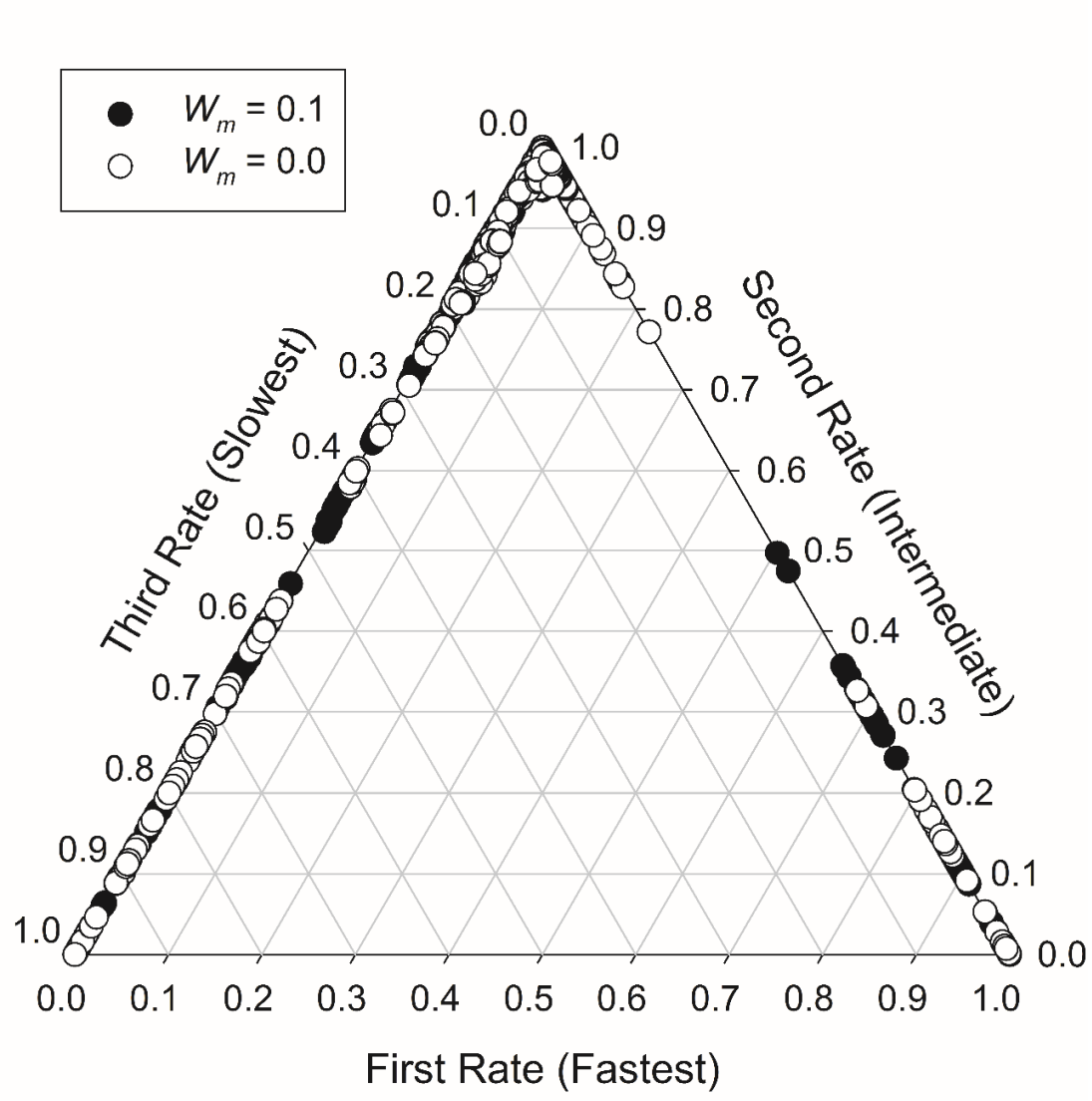

Figure 7: Ternary plot of integrated risks from all profiles in NMRI98 as predicted by the LEM model after optimization with marginal events weighted (W_m = 0.1) and marginal events unweighted (W_m = 0.0) in the training set. Integrated risks for each compartment are normalized by the total integrated risk for the profile. The profile is then plotted on the ternary plot in which each corner represents the situation where all risk came for the compartment whose axis indicates 1.0 in the corner. As each isocline is crossed moving away from a corner the amount of risk contributed by the compartment the 1.0 belongs to decreases by 10%. While profile risks shifted positions, there was no discernable qualitative change in the overall distribution of profile risks.

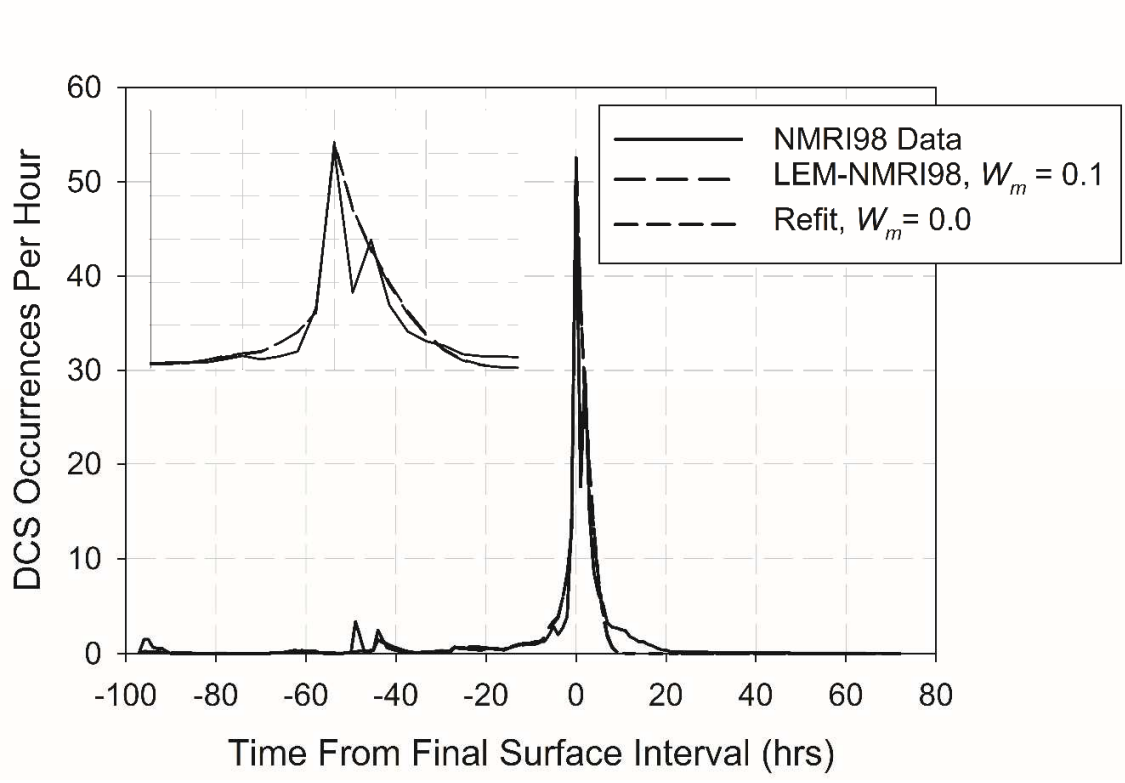

499

500 Figure 8: The occurrence density function (ODF) for the NMRI98 data set. The occurrence density function
501 plots the number of DCS events that either occurred (for the true data) or were expected (model
502 predicted) per hour. The function is centered on the time of surfacing with negative times for DCS
503 occurrences prior to the diver reaching the surface. A zoomed in view of the center of the graph is
504 provided in the top left due to this being where the bulk of the DCS events occur. In the true data, there
505 is a bimodal peak which is not replicated by either of the model parameter sets. The ODFs for LEM
506 optimized with W_m = 0.1 and W_m = 0.0 are indistinguishable at this resolution.

507

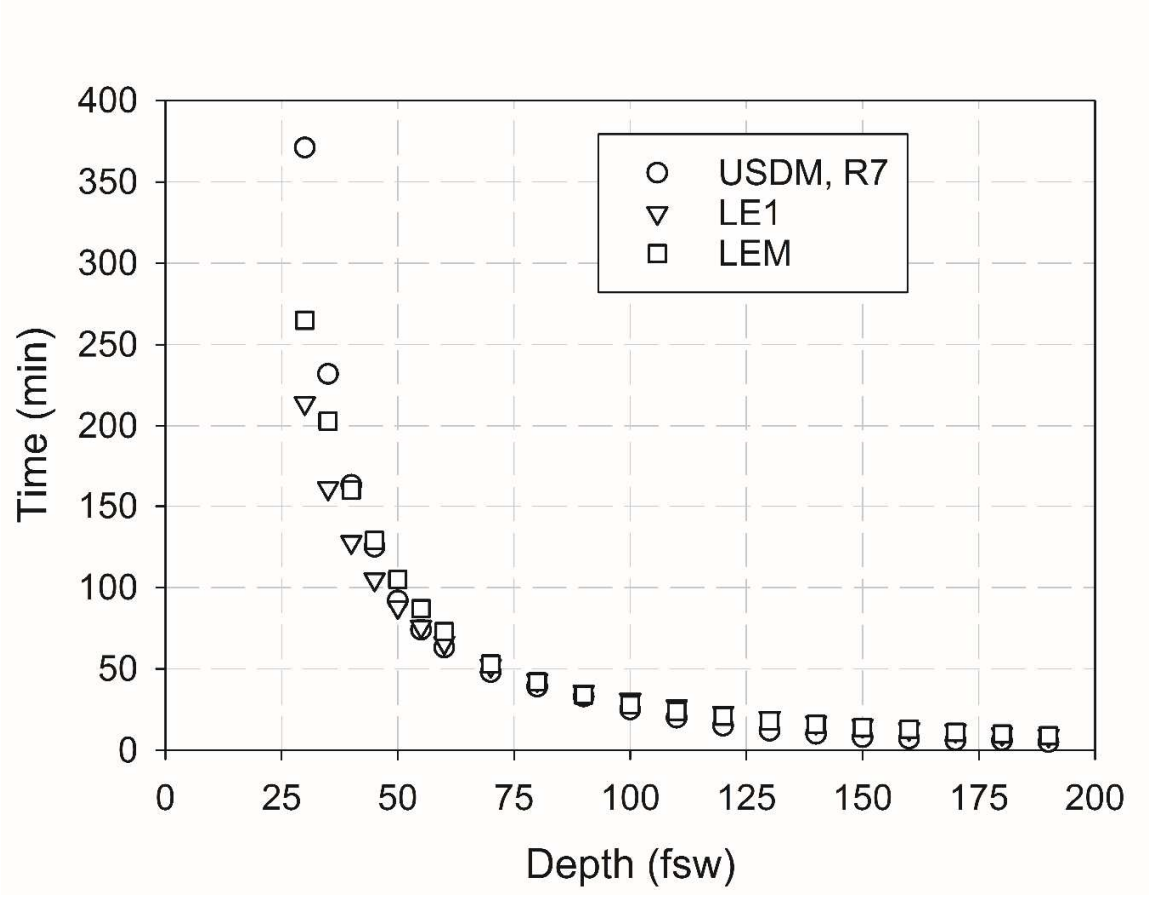

508

509 Figure 9: Air dive no-stop limits published in the USN Dive Manual Revision 7 [46] and the LE1 and LEM
510 models after being refit with W_m = 0.0. All calculations were made assuming air is the inspired gas with a
511 descent rate of 75 fpm and an ascent rate of 30 fpm. Ascent and descent times were not included in the
512 bottom time. Bottom times were increased in increments of 1 minute until a target risk of 2.3% probability
513 of DCS occurring was reached. If 2.3% risk was exceeded the next shorter time was accepted as the limit.

514